

Modeling and quantification of cancer cell invasion through collagen type I matrices

OLIVIER DE WEVER^{*,1}, AN HENDRIX^{#,2}, ASTRID DE BOECK^{#,1}, WENDY WESTBROEK⁴,
GEERT BRAEMS³, SHAHIN EMAMI^{5,6}, MICHÈLE SABBAH⁵, CHRISTIAN GESPACH^{5,6}, and MARC BRACKE¹

¹Laboratory of Experimental Cancer Research, Department of Radiotherapy and Nuclear Medicine, ²Department of Medical Oncology, and ³Department of Gynaecology, Ghent University Hospital, Ghent, Belgium, ⁴National Human Genome Research Institute, NIH, Bethesda, Maryland, USA, ⁵INSERM U 673, Molecular and Clinical Oncology of Human Solid Tumors, ⁶INSERM U938 and Université Pierre et Marie Curie-Paris, Faculté de Médecine, Paris, France

ABSTRACT Tumor invasion is the outcome of a complex interplay between cancer cells and the stromal environment. Considering the contribution of the stromal environment, we developed a membrane-free single-cell and spheroid based complementary model to study cancer invasion through native collagen type-I matrices. Cell morphology is preserved during the assays allowing real time monitoring of invasion-induced changes in cell structure and F-actin organization. Combining these models with computerized quantification permits the calculation of highly reproducible and operator-independent data. These assays are versatile in the use of fluorescent probes and have a flexible kinetic endpoint. Once the optimal experimental conditions are empirically determined, the collagen type-I invasion assays can be used for preclinical validation of small-molecule inhibitors targeting invasion. Initiation and monitoring of the single-cell and spheroid invasion model can be achieved in 8 h (over 3 days) and in 14 h (over 8 days) respectively.

KEY WORDS: *invasion, collagen, stroma, 3D matrices, ecosystem*

Introduction

Emergence of the invasive behavior during cancer progression is a critical feature of malignancy. Several classes of proteins involved in the tethering of cells to their surroundings in a tissue are altered in cells possessing invasive capabilities. The affected proteins include cell-cell adhesion molecules such as members of the calcium-dependent cadherin families, and integrins, which link cells to extracellular matrix substrates. However, molecular and cellular research focused on cancer cells themselves appear to be inadequate since several tumor cell populations including myofibroblasts, bone marrow-derived mesenchymal stem cells, immune and endothelial cells become resident within clinical tumors (De Wever *et al.*, 2007; De Wever *et al.*, 2008). Indeed, according to the multifactorial nature of the malignant transformation, it is generally well accepted that cancer invasion is the outcome of a complex interplay between cancer cells and the host tissue environment in solid tumors (Hanahan and Weinberg, 2000). *In vitro* modeling is appropriate for dissecting various mechanisms involved in cancer cell invasion and stromal cell

infiltration because it can simultaneously and quantitatively integrate the complex interactions between multiple factors and tumor cell populations (De Wever *et al.*, 2004b; Nyström *et al.*, 2005). To study this cell-matrix interaction *in vitro*, several natural extracellular matrix (ECM) types have initially been applied. Bone (Kuettnner *et al.*, 1978), salt-extracted cartilage (Pauli *et al.*, 1981) and amnion membrane (Liotta *et al.*, 1980) are examples of devitalized substrata that have been launched in the past to discriminate between invasive and non-invasive cells. Lack of homogeneity of these substrata often made interpretation of invasion difficult, and hampered the reproducibility of those assays. To overcome these drawbacks reconstituted and hence more homogeneous ECMs were developed, and proposed as substrata to test invasion. Currently, Matrigel (Albini *et al.*, 2007), Humatrix (Kedeshian *et al.*, 1998) and pepsin-extracted or native, acid-extracted collagen type I (Sabeh *et al.*, 2009; Vakaet *et al.*,

Abbreviations used in this paper: ECM, extracellular matrix; GFP, green fluorescent protein.

***Address correspondence to:** Dr. Olivier De Wever. Laboratory of Experimental Cancer Research, Department of Radiotherapy and Nuclear Medicine, Ghent University Hospital, De Pintelaan 185, B-9000 Ghent, Belgium. Tel: +32-9-332-3008. Fax: +32-9-332-4991. e-mail: olivier.dewever@UGent.be

#Note: Both authors contributed equally to this work.

Accepted: 13 August 2009. Final author-corrected PDF published online: 28 August 2009.

1991; Wolf *et al.*, 2003) are frequently used as ECM substrates in invasion assays. The ideal model would allow for easy manipulation, quantification by digital analysis, morphotypic and morphometric studies, further downstream biochemical assays, and close recapitulation of the *in vivo* situation (Bruyère *et al.*, 2008).

The models presented in the present protocol, are based on the preparation of a native collagen type I gel, the main interstitial matrix component in solid tumors, in which the addition of test cell populations either as single-cells on top of the collagen or as cellular spheroid aggregates inside the collagen is varied. The use of multicellular spheroid aggregates allow us to gain insight into therapeutic problems associated with metabolic and proliferative gradients, such as the altered responsiveness and effects of chronically hypoxic tumor cells, and the importance of 3D cell-cell and cell-matrix interactions in radio- and chemoresistance (Friedrich *et al.*, 2009). With the increasingly recognized fact that gene signatures from the stromal environment are critical parameters for tumor progression and clinical outcome (Finak *et al.*, 2008), we need to develop original models to test how stromal-derived structural and biochemical cues drive invasive cancer growth. In the heterotypic spheroid invasion model, the tumor environment is represented by stromal myofibroblasts. During the time course of the assay cell morphology is preserved in the matrix, allowing biochemical analysis and real-time monitoring to acquire important insights into basic features of the invasive migratory process. In a next step, computer-generated binary images allow the calculation of highly reproducible and operator-independent data, such as the invasion area and morphometry. This protocol or parts of this protocol have been used successfully by us and others in the past (Behrens *et al.*, 1993; De Wever *et al.*, 2004a; 2004b; Fritah *et al.*, 2008; Grijelmo *et al.*, 2007; Meerschaert *et al.*, 2007; Mooradian *et al.*, 1992; Nguyen *et al.*, 2005; Nyström *et al.*, 2005; Roperch *et al.*, 2008; Van Aken *et al.*, 2004; Vleminckx *et al.*, 1991). Although it may be impossible to achieve a general standardization of collagen type I invasion models and analysis for all experimental settings, the easy-handling protocols presented herein for single cell and spheroid invasion models, and morphometric analysis are designed to encourage scientists and the pharmaceutical industry to consider (collagen type I) invasion models as part of the standard repertoire for drug evaluation.

Experimental Protocols (I - Reagents, Equipment)

Reagents

The lists provided in this section are based on the materials used in our laboratory. Chemicals and cell culture materials may be purchased from other distributors and/or manufacturers.

- Dulbecco's modified eagle medium (DMEM; Invitrogen cat.no. 41965-039). Store at 4°C.
- FBS (Greiner cat.no. 758093S5595)
Long time storage at -20°C, short term at 4°C.
CRITICAL: Serum quality affects single-cell and spheroid formation and should be routinely tested!
- Penicillin/streptomycin 10,000 U pen./10mg strep. ml⁻¹ (Invitrogen cat.no. 15140163). Store at 4°C.
- Trypsin (0.5% wt/vol) ethylenediaminetetraacetic acid (EDTA; 0.2% wt/vol) solution (Invitrogen cat.no. 25300054-100ml). Store at 4°C.
- Phosphate-buffered saline (PBS; Invitrogen cat.no. 20012019).

Store at 4°C.

- Trypan blue (Sigma cat.no. T8154)
CAUTION: Trypan blue is a possible cancer hazard: wear gloves.
- Native, acid-extracted rat tail collagen type I (BD Biosciences cat.no. 354236). Store at 4°C.
- Calcium- and magnesium-free Hank's balanced salt solution 1x (CMF-HBSS; Sigma cat.no. H6648). Store at 4°C.
- Minimal essential medium (MEM), concentrated 10-fold. (Invitrogen cat.no. 21430-20). Store at 4°C.
- Sodium bicarbonate (Sigma cat.no. S5761)
- Sodium hydroxide (Sigma cat.no. S5881)
CAUTION: Corrosive, wear suitable gloves and eye/face protection.
- Melting ice
- Human recombinant transforming growth factor (TGF)- α (Sigma cat.no. T7924). Store at -20°C.
- Dimethyl sulfoxide (DMSO; Sigma cat.no. D8418).
CAUTION: Hazardous: avoid contact with skin and eyes.
- Gefitinib (kindly provided by AstraZeneca). Store at -20°C.
- Paraformaldehyde (Fluka cat.no. 76240)
- Phosphate-buffered saline with Ca²⁺, Mg²⁺ (PBS^D-Dulbecco's modification-; Invitrogen cat.no. 14040083). Store at 4°C.
- BSA (Sigma cat.no. A4503-500g). Store at 4°C.
- Glycine (Sigma cat.no. G6201)
- Triton X-100 (Biorad cat.no. 161-0407)
- Phalloidin Alexa Fluor 488 and Alexa Fluor 594 (Molecular Probes cat.no. A12379 and A12381). Store at 4°C.
- Mounting medium (GlycerGel; DakoCytomation cat.no. C0563)
- Microscope slides and cover glass (Immuno-Cell; cat.no. 7107 and 1818)

Equipment

- Bürker hemocytometer
- Cell culture plates (6 well multidish plate) (Nunc cat.no. 140675)
- Cell culture flasks T25 and T75 (Greiner Bio-One GmbH cat. nos. 690175 and 658175)
- Centrifuge: Sorvall RT 6000D
- CO₂ incubators (Life Sciences international, Forma Scientific 3111)
- Erlenmeyer (Sigma cat.no. Z723045)
- Gyrotory shaker (New Brunswick Scientific Company cat.no. G-33)
- Microscopes: Inverted phase-contrast microscope equipped with a digital colour camera (Leica Microsystems GmbH cat. nos. DMI 3000B and DFC 340 FX). Fluorescence/phase-contrast motorized inverted Axiovert 200M microscope equipped with an AxioCam HRm camera (Carl Zeiss MicroImaging GmbH cat. no. 426511-9901-000) and a temperature controlled CO₂-incubation system for live cell time-lapse experiments.
Zeiss 510 META confocal laser-scanning microscope using a 488 argon and a 543 HeNe laser. Images are acquired using a Plan Aplanachromat 20X/0.75 or a Plan NeoFluar 40X/1 lens.
- Scalpel and forceps to manage fixed collagen gels
- Software: Axiovision 4.5 (Zeiss); image manager (IM50; Leica); Image J (<http://rsbweb.nih.gov/ij/>); statistical analysis (SPSS)

Reagent setup

Standard medium

DMEM with phenol red containing 4.5g liter⁻¹ D-glucose, 1% (wt/vol) L-glutamine and without sodium pyruvate, supplemented with 100U ml⁻¹ penicillin, 100mg ml⁻¹ streptomycin and 10% FBS is used

as standard medium for routine cell and spheroid culturing and preparation of collagen gels. Standard medium can be stored at 4°C for up to 2 weeks.

Drugs for preclinical validation (e.g. gefitinib)

Prepare appropriate stock solutions of drugs and store at conditions required to keep optimal drug activity. For most but not all drugs in our laboratory, 100mM stock solutions in DMSO and storage at -20°C are suitable. Final DMSO concentrations in the collagen invasion assays of <0.2% are not expected to affect cancer invasion. Minor effects may already be seen at a concentration of 0.2-1%, depending on the cell type and culture condition. A proportion of >1% DMSO in the drug dilution for treatment should be avoided. Other solvents are to be verified. Individual solvent controls for each drug concentration may be considered.

0.25M Sodium bicarbonate

Dissolve 2.2g of sodium bicarbonate in 100ml of CMF-HBSS. Stir until the solution becomes clear, store at 4°C.

1M Sodium hydroxide

Dissolve 4g of sodium hydroxide in 100ml of CMF-HBSS. Stir until the solution becomes clear, store at 4°C.

Human recombinant TGF- α

Add 1ml of sterile PBS containing 0.1%BSA to a vial containing 0.1mg of TGF- α . This makes a a stock solution of 100 μ g ml⁻¹. Prepare 50 μ l aliquots and store at -20°C for up to 6 months.

3% paraformaldehyde

Dissolve 3g of paraformaldehyde in PBS and adjust the volume to 100ml of PBS, heat the mixture to 80°C, stir until the solution becomes clear, add 10 μ l 1M CaCl₂ and 10 μ l 1M MgCl₂ and cool to room temperature and check that the pH=7.4. Filter through a 0.45 μ m filter and use immediately or store aliquots in dark glass bottles in -20°C. Thawed paraformaldehyde should be warmed to at least room temperature or preferable 37°C, discard remaining solution after thawing.

CAUTION Paraformaldehyde is toxic. Work under the hood and use gloves.

2%BSA/1%glycine in PBS

Dissolve 2g BSA and 1g glycine in PBS and adjust the volume to 100ml of PBS, stir until the solution becomes clear, store at 4°C.

0.5% Triton X-100 solution

Add 500 μ l of Triton X-100 to 100ml of PBS.

Experimental Protocols (II - Equipment Setup)

Cancer cell lines

Various cancer cell lines of different origin are subjected to the collagen invasion protocol (Table 1). All of these lines are commercially available (except HCT-8/E11 which is an epithelial subclone from HCT-8 (Vermeulen *et al.*, 1995); the HCT-8/E11 cell line is available from our laboratory upon request). Not all of these can be applied in a spheroid-based screen (Friedrich *et al.*, 2009). All cell lines are cultured in standard medium and transferred using the same trypsin/EDTA working solution. All stocks

have been tested to be free of mycoplasmas, are frozen in 90% FBS plus 10% (vol/vol) DMSO solution and are stored in liquid nitrogen for subsequent reculturing. Cancer cells between passages >2 and <30 are most suitable for use in single-cell and spheroid invasion model. Keep cultures in humidified atmosphere with 10% CO₂ in air at 37°C.

Stromal myofibroblast primary cultures

Isolate primary human colon tumor-derived myofibroblast cells from tumor explants (De Wever *et al.*, 2004a; 2004b). Myofibroblasts at passages >2 and <8 are most suitable for use in the heterotypic spheroid invasion model. Use standard medium for routine culturing. Keep cultures in humidified atmosphere with 10% CO₂ in air at 37°C.

Image processing

Sample preparation, optical microscopy observations and image caption conditions must be carefully established in order to achieve optimal image quality, i.e., a maximum contrast between the sample and the background. However, in some cases, experimental conditions prevent, to fulfill completely this requirement. For example, if the single-cells or spheroids are placed at the border of the support, uneven illumination could generate a dark rim on both sides of the image.

Process and quantify the digital images (300 pixels inch⁻¹) using ImageJ software. Change the image to 8-bit type. Use the threshold function to convert areas of interest to saturated black areas in a uniform manner to have a binary (black&white) image. In a next step, subject the binary image to two 'clean-up' procedures: exclude all particles less than three pixels in size and remove any artifacts by comparing the binary image to the phase-contrast or phase-contrast-GFP fluorescence pictures. Use the set measurements dialog box to specify area and perimeter. Use the analyze particle dialog box to measure all particles and to generate a "particle report" for each image in which the area and perimeter of individual particles and the area of the sum of individual particles is documented. The area calculated as number of pixels is defined as invasion-area in the single-cell invasion

TABLE 1

MORPHOTYPE ANALYSIS OF TISSUE CULTURE PLASTIC SUBSTRATE AND SINGLE CELL INVASION INTO COLLAGEN TYPE I OF 15 COMMERCIALY AVAILABLE HUMAN CANCER CELL LINES

Tumor entity	Cell line	ATCC number	Morphotype	Invasion
Breast	MCF7	HTB-22	E	-
	MDA-MB-231	HTB-26	F	++
	T-47D	HTB-133	E	-
	ZR-75-1	CRL-1500	E	-
Cervix	HeLa	CCL-2	F	+++
Colon	HCT-8/E11	Derived from CCL-244	E	-
	HCT 116	CCL-247	E	-
	HT-29	HTB-38	E	-
	LoVo	CCL-229	E	-
	SW480	CCL-228	M	-
Neuroblastoma	SK-N-SH	HTB-11	F	+++
Osteosarcoma	HT-1080	CCL-121	F	+++
Ovary	SK-OV-3	HTB-77	F	++
Prostate	DU 145	HTB-81	E	-
	PC3	CRL-1435	F	+++

E, epitheloid; F, fibroblastic; M, Mixed; -, 0-4.9%; +, 5-9.9%; ++, 10-14.9%; +++, >15%

assay and as area in the heterotypic spheroid invasion assay. The mean invasion area or area is indicated +/- standard error mean. The shape factor refers to a value that is affected by an object's shape but is independent of its dimensions. Calculate the factor shape from Image J binarized F-actin stainings using the following formula $(\text{perimeter})^2/4\pi(\text{area})$ where $\text{perimeter} = 2\pi R$ and $\text{area} = \pi R^2$. It gives a minimal value of 1 for a perfect circle and larger values for shapes having a higher ratio of perimeter to area (Pinner and Sahai, 2008). The mean factor shape of 30 single-cells or 20 spheroids is indicated +/- standard error mean. The percent fragmentation, used in the heterotypic spheroid invasion model, is calculated as the percent of single or clustered cells released from the total spheroid area. The mean percent fragmentation of 20 spheroids is indicated +/- standard error mean.

Statistics

Perform Chi-Square test for group comparison in the single-cell collagen invasion model when counting the number of non-invasive and invasive cells in 10 microscopic fields.

Use Mann Whitney test when comparing invasion area in the single cell collagen invasion model and factor shape in both invasion models.

Analyze the area data in the heterotypic spheroid collagen invasion model by repeated measures analysis of variance with testing of the equality of variances. Use the Tukey's test for post hoc contrasts.

Experimental Protocols (III - Procedure)

Single-cell collagen invasion model

For schematic see Fig. 1.

Preparation of a collagen gel: Working time 30min, incubation time at least 1h

1) Prepare collagen type I solution with a final concentration of 1 mg ml^{-1} collagen type I by mixing the following precooled (stored at 4°C) components: 4 volumes collagen type I (stock is 3.49 mg ml^{-1}), 5 volumes of CMF-HBSS, 1 volume of MEM (10x), 1 volume of 0.25M NaHCO_3 , 2.65 volumes of standard medium and 0.3 volumes of 1M NaOH to make the solution alkaline.

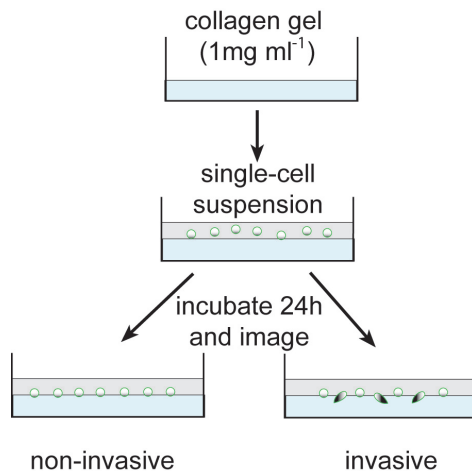


Fig. 1. Schematic of the single-cell invasion model.

CRITICAL: Mix gently by pipetting, avoiding the introduction of air bubbles. Keep the solution on melting ice. The final solution should look purple due to the phenol red pH indicator showing a $\text{pH} > 9$. The concentration of the stock collagen type I is variable. Adapt volume of collagen type I with CMF-HBSS if necessary. Volumes of MEM, NaHCO_3 , standard medium and NaOH remain constant. If necessary, you may increase concentration of collagen type I up to 2 mg ml^{-1} .

TIMING: Collagen type I solution can be stored at 4°C for up to two weeks.

TROUBLESHOOTING advice can be found in Table 2.

2) Add, for each test-condition, 1.25ml of collagen type I solution to one well of a 6-well plate, spread homogeneously and let gelify on a flat surface in a humidified atmosphere of 10% CO_2 in air at 37°C for at least 1h to obtain a collagen gel with a $250 \mu\text{m}$ central thickness in the well.

CRITICAL: Avoid introduction of air bubbles. Monitor the polymerization of the collagen gel carefully before starting step 5-6.

TIMING: You may keep collagen type I gels up to 24h in a humidified atmosphere of 10% CO_2 in air at 37°C .

SUGGESTION: You may add the testing products in collagen type I solution.

TROUBLESHOOTING advice can be found in Table 2.

Preparation of single-cells: Working time 30min

Perform step 3-5 during gelification time of collagen.

3) Prepare a single-cell suspension in standard medium by mild enzymatic dissociation, using a Ca^{2+} - and Mg^{2+} -free PBS wash followed by incubation with a trypsin/EDTA solution, of an exponentially growing culture (usually 70% confluence is used). **CRITICAL:** Optimize trypsinization procedure for every cell type. It is essential to inactivate trypsin and to remove EDTA after trypsin/EDTA procedure. Trypsin inhibition is accomplished by trypsin inhibitors in the serum in the standard medium. Therefore, dilute the suspended cells with 5ml of standard medium and pellet by centrifugation. Aspirate the supernatant, and resuspend the cells in 5ml of standard medium. Repeat this procedure twice.

Avoid cell doublets and clusters by filtering the cell suspensions through $30\text{-}35\mu\text{m}$ sterile meshes or fine needle aspiration (especially when using strongly adherent cell lines such as HCT-8/E11, MCF7 and HT-29). Avoid repeated dissociation of cell cultures within less than 2 d.

4) Count a small aliquot of the cell suspension after staining with Trypan blue (0.04% Trypan blue in PBS) to exclude dead cells.

Initiation of invasion model: Working time 30 min for 6 conditions

5) Prepare $1\text{-}2 \times 10^5$ viable, single-cells in 1ml standard medium in 15ml polypropylene tubes. Add test products such as growth factors (TGF- α) or drugs for preclinical (gefitinib) validation in desired concentration. Gently seed this mixture on top of blind-coded collagen type I gels.

CRITICAL: Avoid high pressure seeding of the cell suspension, it may damage the collagen gel.

Use left-right and forward-backward movement of the 6-well plate to make sure the cells are evenly distributed over the whole gel surface.

TROUBLESHOOTING advice can be found in Table 2.

6) Incubate cells in a humidified atmosphere with 10% CO_2 in

air at 37°C for 24h.

Evaluation of single-cell invasion: Working time 1h for 6 conditions

7) Focus an inverted phase-contrast microscope (with objective 10x or 20x) downwards from the culture medium to the top of the gel onto a single focal plane. The edges of the cells appear brighter (cells have a 'halo' of light) compared to the background. The degree of reduction in brightness depends on the refractive index. Dense structures such as the nucleus or fibrillar collagen appear dark. Cellular extensions invading the collagen matrix appear dark because they are located out of phase (focal plane). Occasionally and dependent from cell-line to cell-line whole single-cells have migrated into the gel and appear dark.

CRITICAL: Choose the first field near the center of the well, consecutive fields are located randomly starting from this central field. Reject fields containing optical artefacts. Use microscope fields with a total of 20-25 cells.

TROUBLESHOOTING advice can be found in Table 2.

8) Take a digital image from 10-15 microscope fields.

Calculation of invasion index (manual cell counting): Working time 1h for 6 conditions

9) Calculate the invasion index (cells with invasive extensions versus total number of cells x 100) by manual counting the number of invading and non-invading cells present in 10-15 microscope fields. Results can be plotted as depicted in Fig. 2.

Calculation of invasion area (digital analysis): Working time 3h for 6 conditions

10) Process image into a binary image to allow computerized

quantification of the invasive extensions. This implicates a two step process. Fig. 2 shows a raw binary image that includes invasive cellular extensions and binary artefacts such as collagen fibers and intracellular structures. Finally, logical subtraction allows to identify the invasive cellular extensions (Fig. 2). The mean invasion area from 10-15 microscopy fields can be calculated by counting the pixel number (Fig. 2).

Evaluation of F-actin cytoskeleton organization: Working time 2h for 6 conditions

11) Fix collagen matrices for 20 min with 3% paraformaldehyde in PBS at room temperature.

TIMING: Fixed matrices can be kept in PBS at 4°C for 2 weeks.

12) Remove a 1cm² surface by scalpel and forceps from the middle of the collagen gel.

TROUBLESHOOTING advice can be found in Table 2.

13) Permeabilize collagen gels for 15 min with 0.5% Triton X-100 in PBS and block for 30 min with 2% BSA/1% glycine in PBS (Denys *et al.*, 2008). Incubate samples for 30min at 37°C with Alexa Fluor 488 or 594 conjugated phalloidin, followed by extensive washing and mounting.

CRITICAL: Always keep samples in the dark when using fluor dye conjugated phalloidin. Solidify mounting medium on a cold plate.

Fix edges of cover glass with nailpolish to avoid movement during microscopy.

14) Cells are imaged by confocal laser-scanning microscopy using a 488 argon or a 543 HeNe laser. Images are acquired using a Plan NeoFluar 40X/1 lens.

Calculation of factor shape: Working time 1h for 30 cells

15) Process image into a binary image to allow computerized

TABLE 2

TROUBLESHOOTING TABLE OF SINGLE CELL COLLAGEN INVASION MODEL

Step	Problem	Possible reason	Solution/action
1	Formation of precipitate during mixing of solutions	The mix is too alkaline	Reduce volume of NaOH
	Air bubbles in solution	High pressure pipetting	Pipet gently Remove air bubbles by centrifugation and careful aspiration of bubbles by pipetting
	Polymerization of solution	High temperature	Keep solution on melting ice
6	Inhomogeneous distribution of single cells over collagen surface	Unefficient shaking	Use left-right and forward-backward movements, do not use circular movements of 6-well plate Check homogeneous distribution of cells by phase-contrast microscopy after cell seeding and shaking
	Cell doublets or islands instead of single cells	Unefficient trypsinization procedure	Optimize trypsinization procedure Avoid cell doublets and clusters by filtering the cell suspensions through 30-35µm sterile meshes or fine needle aspiration
	Floating collagen gel	High pressure seeding of cells Plates were disturbed during incubation	Gently pipet single cell suspension along the side of the well plate on the collagen gel Never slam doors of the respective and adjacent incubators If feasible, use separate incubator for incubation to elude frequent openings
	Dissolved collagen gel	Use of hypertonic solutions	Check osmolality of test products Make test products isotonic
8	Impossibility to find superficial cells	Highly invasive cells make it difficult to discern the top of the collagen gel	Add carbon particles, they remain on top of the collagen gel and will not invade into the collagen
		Too many floating cells	Remove floating cells Check toxicity of test product
	Presence of debris or small particles	Superficial cells are deeper on one side of the microscope field compared to the other side	The surface of a gel is not always completely flat, choose therefore another field Avoid cell counting at the periphery (1cm) of the well, because here meniscus formation of the collagen can disturb the top level of the gel, and can contain fewer cells due to rolling towards the more central parts.
		Small particles in standard medium and/or serum	Monitor media and filter supplemented media through sterile filter if required
Dynamics of invasion		Perform time lapse video recordings using Axiovert 200M equipped with temperature controlled CO ₂ -incubation system	
13	Destruction of collagen gel while cutting	Unefficient fixation	Fix 20 min, 3% paraformaldehyde at room temperature
		Climsy cutting and forceps handling	Increase your handiness and experience on "try-out" collagen gels

quantification of perimeter and area of 30 imaged cells and calculate factor shape.

Heterotypic spheroid collagen invasion model

For schematic see Fig. 3.

Spheroid initiation: Working time 1h

1) Prepare a single-cell suspension (see step 3 single-cell invasion model).

CRITICAL: Use cancer cells transfected with reporters such as GFP or DsRed for optimal contrast between cancer cell spheroid and collagen gel during image analysis.

2) To initiate compact spheroids of 150- μm diameter at day 3 after inoculation, dilute dissociated cells to appropriate concentrations in 6ml standard medium, e.g. 2×10^5 cells ml^{-1} for HCT-8/E11-GFP human colon cancer cells, in a 50-ml Erlenmeyer flask. This cell number is sufficient to obtain +/-100 compact spheroids of 150- μm diameter.

CRITICAL: For each cancer cell line, the cell number that is needed to create spheroids of +/-150 μm in diameter at day 3 after initiation has to be determined empirically (Friedrich *et al.*, 2009). In our setup, compact spheroid formation is routinely checked by individual microscopic evaluation for cell concentrations ranging from 5×10^4 to 5×10^5 cells ml^{-1} .

TROUBLESHOOTING advice can be found in Table 3.

3) Incubate Erlenmeyer flasks for 72 h on a Gyrotory shaker at 37°C and 70 rpm in humidified atmosphere with 10% CO_2 in air.

TROUBLESHOOTING advice can be found in Table 3.

4) After 72 h of incubation (day 3 after initiation of spheroids) control sphericity and compaction of spheroids by individual microscopic monitoring (x-y-z direction).

If spheroids are spheric and compacted proceed with step 7.

CRITICAL: Avoid precipitation and/or attachment of spheroids on glass substrate. Replace Erlenmeyer containing spheroids on a Gyrotory shaker at 37°C and 70 rpm in humidified atmosphere with 10% CO_2 in air, when quality control is microscopically evaluated.

TROUBLESHOOTING advice can be found in Table 3.

Preparation of collagen type I bottom gellayer (eventually containing stromal cell population): Working time 30min, incubation time 1h

5) Prepare a single-cell suspension from primary myofibroblasts cultured in standard medium by mild enzymatic dissociation, using a Ca^{2+} - and Mg^{2+} -free PBS wash followed by incubation with a trypsin/EDTA solution (usually 70% confluence is used).

CRITICAL

See step 3 single-cell collagen invasion model.

6) Prepare collagen type I solution (see step 1 of single-cell collagen invasion model).

7) Prepare 1×10^6 viable, single myofibroblasts in 1.25ml collagen type I solution and pour gently in a well of 6-well plate. For control use 1.25ml of collagen type I solution without myofibroblasts.

CRITICAL: Use left-right and forward-backward movement of the 6-well plate to make sure the cells are evenly distributed in the whole gel solution.

8) Incubate collagen gels in a humidified atmosphere with 10% CO_2 in air at 37°C for 1h.

Preparation of spheroid-containing collagen type I gellayer: Working time 1h, incubation time 1h

Perform step 9-10 during gelification time of bottom collagen type I layer.

9) Transfer approximately 20 spheroids (a volume of 1.20ml) in a 15ml polypropylene tube. Let the spheroids sediment through gravitation.

CRITICAL: Do not centrifuge spheroids, they may stick together to form one large aggregate.

10) Discard the supernatant and add 1.25ml of collagen type I solution. Mix gently, avoid the introduction of air bubbles and pour gently onto existing collagen type I layer.

CRITICAL: Avoid high shear stress by pipetting, it may damage-desintegrate the spheroids. Use left-right and forward-backward movement of the 6-well plate to make sure the spheroids are evenly distributed in the whole gel solution.

TROUBLESHOOTING advice can be found in Table 3.

TABLE 3

TROUBLESHOOTING TABLE OF HETEROTYPIC SPHEROID COLLAGEN INVASION MODEL

Step	Problem	Possible reason	Solution/action
1-4	Formation of irregular, noncircular spheroids	Use of cell suspension containing too many cell clusters/doublets	Optimize trypsinization procedure Avoid cell doublets and clusters by filtering the cell suspensions through 30-35 μm sterile meshes or fine needle aspiration
		Small particles in medium and/or serum	Check cleanliness of beakers and of any other reusable glass or plastic materials Monitor standard media and filter through sterile filter if required Carefully aliquot heat-inactivated serum to omit solid particles
	Formation of loose cell aggregates of compact spheroid-forming cell lines	Disordered aggregation of cells either after thawing or at high passages or due to mycoplasma contamination Incorrect incubation conditions	Transfer stock solutions at least twice after thawing and before spheroid initiation Trash morphologically altered cells and renew stock cultures from frozen backup Check regularly for mycoplasma contamination, trash culture if positive Check incubator settings and CO_2 connections
	No spheroid formation or formation of loose cell aggregates	Non-compacting or non-aggregating cell line	e.g., MDA-MB-231 breast cancer cells do not form compact spheroid but loose cell aggregates. This cell line is not suitable in the spheroid invasion assay
	Spheroids are attached to bottom of Erlenmeyer	Shaking was disturbed	Do not stop Gyrotory shaker during spheroid initiation Be aware of power breaks during spheroid initiation
11-12	Detachment of second layer from first layer	Incubation time for gelification of second collagen layer was too short	Increase incubation time, at least 1h
		High pressure pipetting of standard medium on second collagen layer	Pipet gently

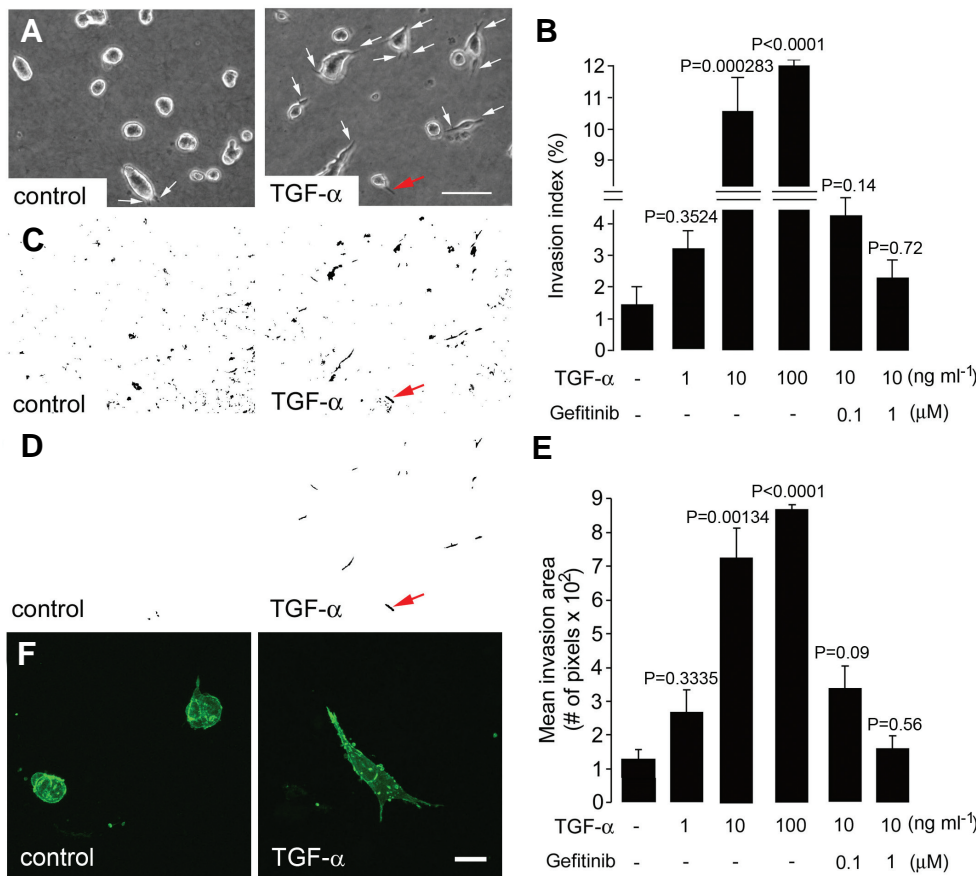


Fig. 2. Representative data of a single-cell collagen invasion assay. (A) Phase contrast pictures of single HCT-8/E11 colon cancer cells seeded on collagen type I gel and cultured for 24 h in culture medium or culture medium supplemented with TGF- α (10 ng ml⁻¹). Arrows indicate invasive extensions. Scale bar, 20 μ m. (B) Quantification of collagen invasion by calculating the invasion index which is the ratio of the number of cells containing invasive extensions over the total number of cells counted in each field, for a total of 10 fields. (C) Computerized binary image processing of phase contrast pictures. (D) Processed binary image by logical subtraction of artefacts such as dense collagen fibres and nuclei. In (A, C, D), the red arrow shows consecutive focusing of one invasive extension in phase contrast picture, unprocessed binary image and logical subtracted binary image. (E) Quantification of the invasion area by counting the number of pixels by computerized Image J analysis. (F) Confocal images of representative phalloidin-Alexa Fluor 488 stained HCT-8/E11 cells cultured for 24 h on collagen type I. Arrows indicate spreaded cells with formation of cellular extensions. Scale bar, 20 μ m.

11) Incubate in a humidified atmosphere with 10% CO₂ in air at 37°C for 1 h to allow gelification of collagen solution. TROUBLESHOOTING advice can be found in Table 3.

12) Code all individual spheroids by numbering them with a pen on the bottom of the well plate. Add 2 ml of standard medium, refresh every 48 h and incubate in a humidified atmosphere with 10% CO₂ in air at 37°C.

CRITICAL: Avoid high pressure addition (and exchange) of standard medium, it may damage the collagen gel.

Avoid aspiration of medium but gently remove medium by pipetting.

TROUBLESHOOTING advice can be found in Table 3.

Evaluation of spheroid invasion: Working time 1 h per condition, every day over a period of 4 days

13) Collect phase-contrast GFP images of all individual spheroids at start of incubation and every 24 h thereafter e.g.,

on a Zeiss Axiovert 200 with objective 10x equipped with camera system.

Calculation of area, factor shape, and percentage fragmentation by digital analysis: Working time 1 h for 20 images

14) Process phase-contrast GFP images into a binary image to allow computerized quantification. Analyse the number of pixels and calculate the mean area and perimeter of 20 spheroids by Image J (Fig. 4B and 4D). Calculate factor shape and percentage fragmentation (Fig. 4C).

Evaluation of F-actin cytoskeleton organization: Working time 1 h for 2 conditions

See step 11-14 in single-cell collagen invasion model.

Results and Discussion

Single-cell collagen invasion model

Critical to the integration of the single-cell collagen invasion model into testing protocols of pro- or anti-invasive compounds is the selection of suitable cell lines. Therefore, 15 established, commercially available human cancer cell lines derived from different tumor types are characterized for their morphotype on tissue culture substrate and single-cell invasion into collagen type I (Table 1). For example, HCT-8/E11 cells seeded on top of collagen type I gels, mostly attach as round cells on the collagen with the appearance of a bright halo when cells are in phase (Fig. 2). Occasionally, formation of invasive cellular extensions with a dark appearance is observed. The single-cell invasion model is further validated by evaluating the impact of recombinant TGF- α , a well-recognized pro-invasive growth factor activating the EGF receptor (Rodrigues *et al.*, 2003). As expected, HCT-8/E11 cells supplemented with TGF- α show a tremendous change in morphotype. When TGF- α -treated HCT-8/E11 cells are in phase, multiple cells show a bright halo with dark, cellular extensions (Fig. 2) that are out of phase and actually located inside the collagen matrix. Treatment with TGF- α stimulates the invasive potential of HCT-8/E11 cells in a dose-dependent manner (Chi Square test; 1 ng ml⁻¹, P=0.3524; 10 ng ml⁻¹, P=0.000283; 100 ng ml⁻¹, P<0.0001) (Fig. 2). Accordingly, a clinically approved inhibitor of the EGF receptor, gefitinib, abrogates the TGF- α -stimulated invasion in a dose-dependent manner (Chi Square test; 10 ng ml⁻¹ TGF- α combined with 0.1 μ M gefitinib, P=0.14; 10 ng ml⁻¹ TGF- α combined with 1 μ M gefitinib, P=0.72). Alternatively to manual cell counting, binary

image processing allows computerized quantification of the invasive extensions (Fig. 2). The mean invasion area can be calculated by counting the pixel number of the dark-appearing cellular extensions (Fig. 2), which is significantly higher when HCT-8/E11 cells are supplemented with increasing concentrations of TGF- α (Mann Whitney test; 1ng ml⁻¹, P=0.3335; 10ng ml⁻¹, P=0.000134; 100ng ml⁻¹, P<0.0001). As expected, gefitinib blocked TGF- α stimulated invasion (Mann Whitney test; 10ng ml⁻¹ TGF- α combined with 0.1 μ M gefitinib, P=0.09; 10ng ml⁻¹ TGF- α combined with 1 μ M gefitinib, P=0.56). Cell viability check by Trypan blue exclusion at the end of the experiment showed that this inhibitor did not exert a toxic effect (not shown). The standard deviation of HCT-8/E11 single-cell invasion is reproducibly below 10% between different experiments. Subsequently, the effect of TGF- α on organisation of the F-actin cytoskeleton is investigated on individual HCT-8/E11 cells (Fig. 2). Approximately 99% of control cells have a rounded morphology with prominent cortical (associated with plasmamembrane) F-actin and membrane blebs. Addition of TGF- α disrupts the cortical F-actin in many cells and produces a more elongated cell morphology with multiple long protrusions. In agreement, the factor shape for control cells has a mean of 1.6 +/- 0.6, indicating that they are generally rounded, whereas TGF- α treated cells have increased mean values of 5.9 +/- 1.3 (Mann Whitney test; P<0.0001).

Heterotypic spheroid collagen invasion model

A possible disadvantage of the single-cell invasion assay is that it lacks structural architecture and that the cells are added under a mono-dispersed state. The multicellular spheroid system is much more adapted to study invasion mechanisms taking into account homotypic cell-cell contacts. The spheroid invasion model also reproduces some aspects of the restrictions in cellular growth and viability observed in growing tumors *in vivo*. Growing spheroids *in vitro* mimic growing tumors *in vivo* and their associated progressive deprivation in oxygen (hypoxia), nutrients, growth factors as

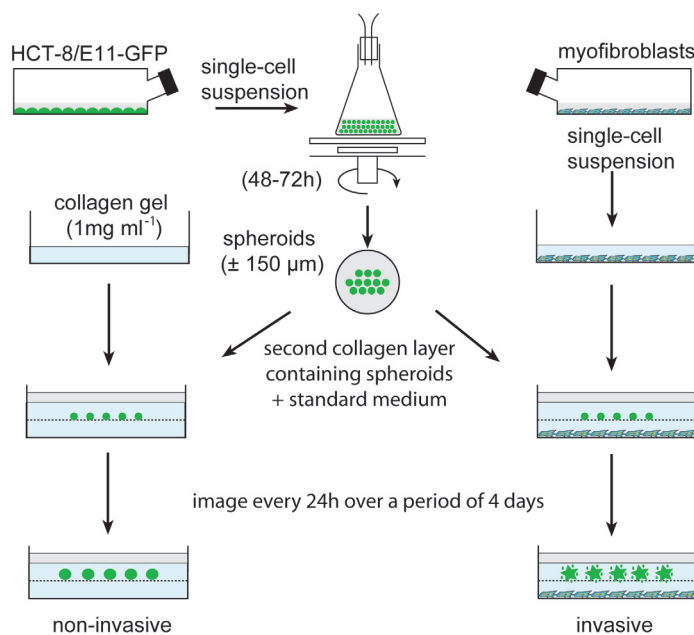


Fig. 3. Schematic of the heterotypic spheroid invasion model.

well as limitations in the penetration and action of drugs. According to literature data, it is expected to identify drug candidates with less therapeutic efficacy in the heterotypic spheroid invasion model (Friedrich *et al.*, 2009). Furthermore, a stromal-derived 50-gene signature predicts resistance to preoperative chemotherapy (5 fluorouracil, epirubicin, cyclophosphamide) in estrogen receptor-negative breast cancer (Farmer *et al.*, 2009). Here, co-culture spheroids will be a tool for negative selection and could (i) contribute significantly to a reduction in animal testings and thus to economical savings and (ii) also become a powerful model to optimize drug candidates for enhanced efficacy. Conversely, there is also experimental evidence that some drugs may exclusively be effective in three-dimensional but not two-dimensional culture, as has been seen in some target-specific treatment modalities, often with the molecular target being expressed only or particularly in a three-dimensional environment (Wang *et al.*, 2002). The co-culture setup of colon cancer cells with colon tumor-derived myofibroblasts in the heterotypic spheroid invasion model allows for investigation of the intimate cellular and molecular cross-signaling between tumor-associated host cells and cancer cells. A representative phase contrast-GFP picture of one HCT-8/E11-GFP spheroid is shown at different time intervals (Fig. 4A). Under control conditions it is obvious that the cancer cell spheroid increases in volume over time but remains shaped as a compact spheric structure. In sharp contrast, the cancer cell spheroid in co-culture with human colon myofibroblasts has a robust increase in volume, is irregularly shaped at the surface circumference, and is fragmented. The cross-signaling with myofibroblasts induces an invasive growth program in HCT-8/E11 colon cancer cells. This invasive growth program (Fig. 4B) is characterized by the factor shape, the percent fragmentation and the mean area calculated from 20 spheroids at each time point. The factor shape has a mean value of 1.3 +/- 0.2 at time 0h indicating the circularity. Under control conditions this value reaches a maximum mean value of 2.84 +/- 0.4 at time 96h, still indicating that the spheroid shape is generally retained (Fig. 4C). Under co-culture conditions this value reaches a maximum mean value of 9.41 +/- 0.85 at time 96h (Mann Whitney test; P=0.000347), indicating the irregular, infiltrating shape of the spheroid. The percent fragmentation remains lower than 1% under control conditions and does not vary with time (Fig. 4C). However, starting after 48h of heterotypic signalling with myofibroblasts, fragmentation is 3-fold stimulated and this fragmentation remains persistent. The size of the patterned spheroid structure is calculated as mean area and is significantly higher starting 24h after co-culture with myofibroblasts as shown in Fig. 4D (repeated measures ANOVA test, P<0.001).

Perhaps the most challenging aspect of complex co-culture studies is to define the phenotypic composition of the growing spheroids. Phenotyping with specific molecular markers, e.g., for cell-cell adhesion (E-cadherin), proliferation (Ki-67), apoptosis (TUNEL) and motility (F-actin), could be done by conventional immuno-histochemical methods on paraffin sections and 3D staining by confocal microscopy in order to connect phenotypes and their relative dominance with tumor morphology. Investigation of the F-actin organization by confocal microscopy reveals that the control spheroids are smoothly edged with occasional formation of invasive extensions (Fig. 4E). However, in the myofibroblast co-culture the spheroid structure has a rough surface and shows fragmented cells inside the collagen matrix. This roughness re-

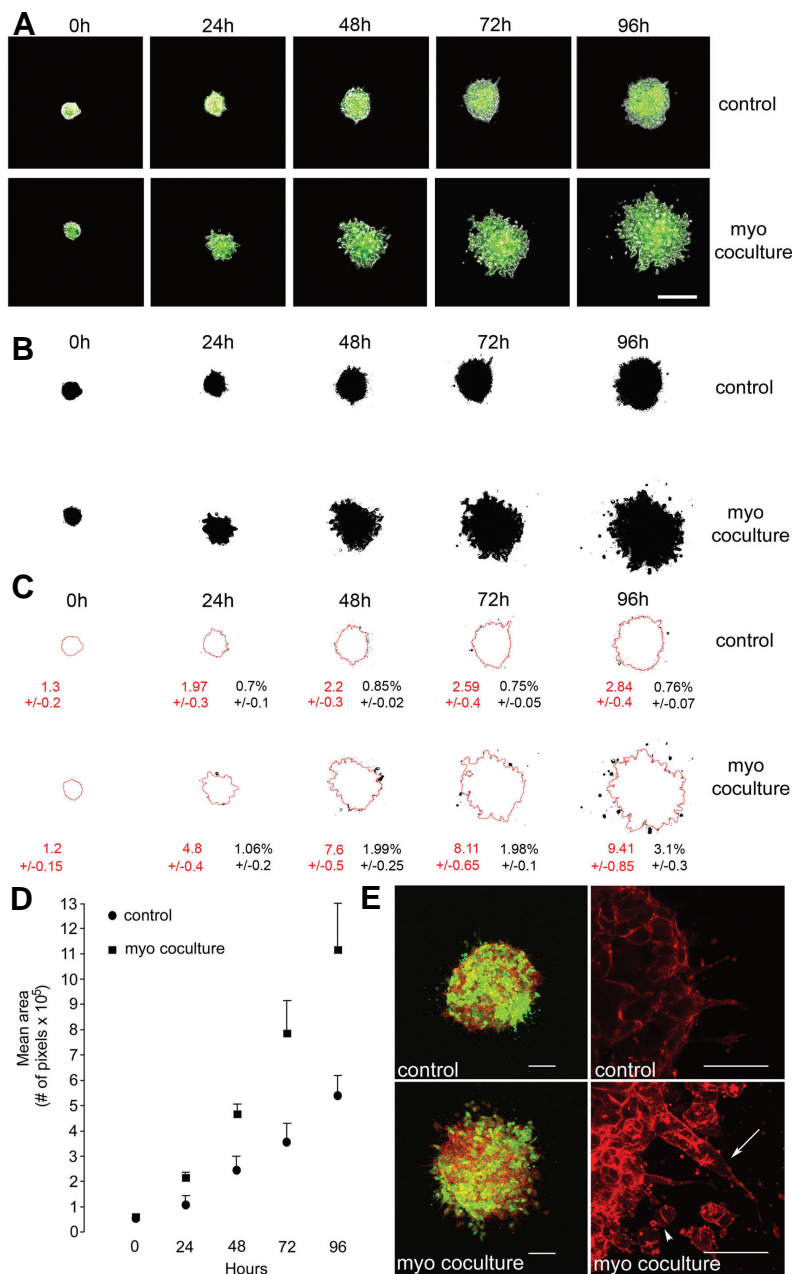


Fig. 4. Representative data of a heterotypic spheroid collagen invasion assay.

(A) GFP-phase contrast pictures of a representative HCT-8/E11-GFP colon cancer cell spheroid followed at different time intervals under control conditions and myofibroblast coculture conditions. Scale bar, 300 μm . (B) Computerized binary image processing of GFP-phase contrast pictures. (C) Factor shape (S) is calculated from $\text{perimeter}^2/4\pi \text{ area}$ and is shown in red \pm s.e.m. A higher number means a more irregular, infiltrating spheroid structure. Fragmentation (%) is calculated from released cells or clusters/total area $\times 100$ and is shown in black \pm s.e.m. (D) Quantification of the area by counting the number of pixels by computerized Image J analysis. Spheroids were followed over time to calculate the morphometric data. (E) Confocal images of representative phalloidin-Alexa Fluor 594 stained HCT-8/E11-GFP spheroids cultured for 96 h under control or myofibroblast coculture conditions. The control spheroid is smoothly edged with occasionally the formation of an invasive protrusion. In the myofibroblast coculture the spheroid edge is fragmented with formation of invasive cells. The arrowhead shows fragmented cells extending short pseudopods inside the collagen matrix. The arrow shows an extension still attached with the main spheroid. Scale bars: left, 75 μm ; right, 50 μm .

flects invasive morphology and can be clearly appreciated by the confocal images of the F-actin staining.

In order to translate the findings from basic cellular research into clinical applications, cell-based models need to recapitulate both the three-dimensional organization and multicellular complexity of an organ but at the same time accommodate systematic experimental intervention. The invasion models, presented here, consist of native collagen type I containing nonhelical telopeptides situated at the N- and C-terminal ends. These telopeptides play an important role in intermolecular covalent cross-links necessary for a gel architecture presenting itself as a structural barrier to cancer cell traffic (Sabeh *et al.*, 2009). These systems allow (i) analysis of pro-/anti-invasive compounds, (ii) analysis of gene dosage/knock down on invasion, (iii) identification of specific mechanisms that underlie invasion, (iv) and analysis of the impact of the stromal environment on cancer invasion. Furthermore, the complementary assays are membrane-free and preserve cell morphology, allow real-time monitoring, have a kinetic flexibility and are highly reproducible. For example, in Transwell[®] chemoinvasion assays where cancer cells invade through a polycarbonate filter coated with a matrix substrate toward a chemoattractant, the number of cells crossing the filter can be counted at various time points. However, when invaded cells attach to the underside of the polycarbonate filter the possibility to perform morphotypic and morphometric analysis is greatly compromised. The collagen invasion models in combination with computerized quantification and powerful cell-pattern-recognition software are cost-effective and offer unprecedented potential for gaining new insights into cancer cell invasion. In support of this, a multiscale mathematical model of cancer invasion, which considers cellular and microenvironmental factors simultaneously and interactively, was developed to provide a theoretical and experimental framework to quantitatively characterize selective pressure for invasion (Anderson *et al.*, 2006). The collagen invasion models, though not an exact replication of the *in vivo* environment, have many obvious applications especially in cancer research but also in tissue engineering and regenerative medicine (Narine *et al.*, 2006).

Acknowledgements

M. Mareel is gratefully acknowledged for stimulating discussions. We thank Georges De Bruyne for excellent technical assistance. This work was funded by Fund for Scientific Research-Flanders (Kornop Tegen Kanker-VLK: FWOAL455) (Brussels, Belgium), INSERM, ARC and the Scientific Exchange Program between the Flemish community and France (Grant I.2007.03; T2009.14). O. De Wever was supported by an EACR travel fellowship, and a post-doctoral grant from Fund for Scientific Research-Flanders. W. Westbroek was supported by the Intramural Research Program of the National Human Genome Research Institute.

References

ALBINI, A. and BENELLI, R. (2007). The chemoinvasion assay: a method to assess tumor and endothelial cell invasion and its modulation. *Nat Protoc* 2: 504-511.

- ANDERSON, A.R.A., WEAVER, A.M., CUMMINGS, P.T. and QUARANTA, V. (2006). Tumor morphology and phenotypic evolution driven by selective pressure from the microenvironment. *Cell* 127: 905-915.
- BEHRENS, J., VAKAET, L., FRIIS, R., WINTERHAGER, E., VAN ROY, F., MAREEL, M.M. and BIRCHMEIER, W. (1993). Loss of epithelial differentiation and gain of invasiveness correlates with tyrosine phosphorylation of the E-cadherin/ β -catenin complex in cells transformed with a temperature-sensitive *v-src* gene. *J Cell Biol* 120: 757-766.
- BRUYÈRE, F., MELEN-LAMALLE, L., BLACHER, S., ROLAND, G., THIRY, M., MOONS, L., FRANKENNE, F., CARMELIET, P., ALITALO, K., LIBERT, C., SLEEMAN, J.P., FOIDART, J.-M. and NOËL, A. (2008). Modeling lymphangiogenesis in a three-dimensional culture system. *Nat Methods* 5: 431-437.
- DE WEVER, O., DERYCKE, L., HENDRIX, A., DE MEERLEER, G., GODEAU, F., DEPYPERE, H. and BRACKE, M. (2007). Soluble cadherins as cancer biomarkers. *Clin Exp Metastasis* 24: 685-697.
- DE WEVER, O., NGUYEN, Q.-D., VAN HOORDE, L., BRACKE, M., BRUYNEEL, E., GESPACH, C. and MAREEL, M. (2004a). Tenascin-C and SF/HGF produced by myofibroblasts *in vitro* provide convergent pro-invasive signals to human colon cancer cells through RhoA and Rac. *FASEB J* 18: 1016-1018.
- DE WEVER, O., WESTBROEK, W., VERLOES, A., BLOEMEN, N., BRACKE, M., GESPACH, C., BRUYNEEL, E. and MAREEL, M. (2004b). Critical role of N-cadherin in myofibroblast invasion and migration *in vitro* stimulated by colon-cancer-cell-derived TGF- β or wounding. *J Cell Sci* 117: 4691-4703.
- DENYS, H., DERYCKE, L., HENDRIX, A., WESTBROEK, W., GHELDOLF, A., NARINE, K., PAUWELS, P., GESPACH, C., BRACKE, M. and DE WEVER, O. (2008). Differential impact of TGF- β and EGF on fibroblast differentiation and invasion reciprocally promotes colon cancer cell invasion. *Cancer Lett* 266: 263-274.
- FARMER, P., BONNEFOI, H., ANDERLE, P., CAMERON, D., WIRAPATI, P., BECETTE, V., ANDRÉ, S., PICCART, M., CAMPONE, M., BRAIN, E., MACGROGAN, G., PETIT, T., JASSEM, J., BIBEAU, F., BLOT, E., BOGAERTS, J., AGUET, M., BERGH, J., IGGO, R. and DELORENZI, M. (2009). A stroma-related gene signature predicts resistance to neoadjuvant chemotherapy in breast cancer. *Nat Med* 15: 68-74.
- FINAK, G., BERTOS, N., PEPIN, F., SADEKOVA, S., SOULEIMANOVA, M., ZHAO, H., CHEN, H., OMEROGU, G., METERISSIAN, S., OMEROGU, A., HALLETT, M. and PARK, M. (2008). Stromal gene expression predicts clinical outcome in breast cancer. *Nat Med* 14: 518-527.
- FRIEDRICH, J., SEIDEL, C., EBNER, R. and KUNZ-SCHUGHART, L.A. (2009). Spheroid-based drug screen: considerations and practical approach. *Nat Protoc* 4: 309-324.
- FRITAH, A., SAUCIER, C., DE WEVER, O., BRACKE, M., BIÈCHE, I., LIDEREAU, R., GESPACH, C., DROUOT, S., REDEUILH, G. and SABBAH, M. (2008). Role of *WISP-2/CCN5* in the maintenance of a differentiated and noninvasive phenotype in human breast cancer cells. *Mol Cell Biol* 28: 1114-1123.
- GRIJELMO, C., RODRIGUE, C., SVRCEK, M., BRUYNEEL, E., HENDRIX, A., DE WEVER, O. and GESPACH, C. (2007). Proinvasive activity of BMP-7 through SMAD4/src-independent and ERK/Rac/JNK-dependent signaling pathways in colon cancer cells. *Cell Signal* 19: 1722-1732.
- HANAHAN, D. and WEINBERG, R.A. (2000). The hallmarks of cancer. *Cell* 100: 57-70.
- KEDESHIAN, P., STERNLICHT, M.D., NGUYEN, M., SHAO, Z.-M. and BARSKY, S.H. (1998). *Humatrix*, a novel myoepithelial matrigel with unique biochemical and biological properties. *Cancer Lett* 123: 215-226.
- KUETTNER, K.E., PAULI, B.U. and SOBLE, L. (1978). Morphological studies on the resistance of cartilage to invasion by osteosarcoma cells *in vitro* and *in vivo*. *Cancer Res* 38: 277-287.
- LIOTTA, L.A., LEE, C.W. and MORAKIS, D.J. (1980). New method for preparing large surfaces of intact human basement membrane for tumor invasion studies. *Cancer Lett* 11: 141-152.
- MEERSCHAERT, K., BRUYNEEL, E., DE WEVER, O., VAN LOO, B., BOUCHERIE, C., BRACKE, M., VANDEKERCKHOVE, J. and GETTEMANS, J. (2007). The tandem PDZ domains of syntenin promote cell invasion. *Exp Cell Res* 313: 1790-1804.
- MOORADIAN, D.L., MCCARTHY, J.B., KOMANDURI, K.V. and FURCHT, L.T. (1992). Effects of transforming growth factor- β 1 on human pulmonary adenocarcinoma cell adhesion, motility, and invasion *in vitro*. *J Natl Cancer Inst* 84: 523-527.
- NARINE, K., DE WEVER, O., VAN VALCKENBORGH, D., FRANCOIS, K., BRACKE, M., DESMET, S., MAREEL, M. and VAN NOOTEN, G. (2006). Growth factor modulation of fibroblast proliferation, differentiation, and invasion: implications for tissue valve engineering. *Tissue Eng* 12: 2707-2716.
- NGUYEN, Q.-D., DE WEVER, O., BRUYNEEL, E., HENDRIX, A., XIE, W.-Z., LOMBET, A., LEIBL, M., MAREEL, M., GIESELER, F., BRACKE, M. and GESPACH, C. (2005). Commutators of PAR-1 signaling in cancer cell invasion reveal an essential role of the Rho-Rho kinase axis and tumor microenvironment. *Oncogene* 24: 8240-8251.
- NYSTRÖM, M.L., THOMAS, G.J., STONE, M., MACKENZIE, I.C., HART, I.R. and MARSHALL, J.F. (2005). Development of a quantitative method to analyse tumour cell invasion in organotypic culture. *J Pathol* 205: 468-475.
- PAULI, B.U., MEMOLI, V.A. and KUETTNER, K.E. (1981). *In vitro* determination of tumor invasiveness using extracted hyaline cartilage. *Cancer Res* 41: 2084-2091.
- PINNER, S. and SAHAI, E. (2008). PDK1 regulates cancer cell motility by antagonising inhibition of ROCK1 by RhoE. *Nat Cell Biol* 10: 127-137.
- RODRIGUES, S., VAN AKEN, E., VAN BOCXLAER, S., ATTOUB, S., NGUYEN, Q.-D., BRUYNEEL, E., WESTLEY, B.R., MAY, F.E.B., THIM, L., MAREEL, M., GESPACH, C. and EMAMI, S. (2003). Trefoil peptides as proangiogenic factors *in vivo* and *in vitro*: implication of cyclooxygenase-2 and EGF receptor signaling. *FASEB J* 17: 7-16.
- ROPERCH, J.-P., EL QUADRANI, K., HENDRIX, A., EMAMI, S., DE WEVER, O., MELINO, G. and GESPACH, C. (2008). Netrin-1 induces apoptosis in human cervical tumor cells via the TAp73 α tumor suppressor. *Cancer Res* 68: 8231-8239.
- SABEH, F., SHIMIZU-HIROTA, R. and WEISS, S.J. (2009). Protease-dependent versus -independent cancer cell invasion programs: three-dimensional amoeboid movement revisited. *J Cell Biol* 185: 11-19.
- VAKAET, L. Jr, VLEMINCKX, K., VAN ROY, F. and MAREEL, M. (1991). Numerical evaluation of the invasion of closely related cell lines into collagen type I gels. *Invasion Metastasis* 11: 249-260.
- VAN AKEN, E.H., DE WEVER, O., VAN HOORDE, L., BRUYNEEL, E., DE LAEY, J.-J. and MAREEL, M.M. (2003). Invasion of retinal pigment epithelial cells: N-cadherin, hepatocyte growth factor, and focal adhesion kinase. *Invest Ophthalmol Vis Sci* 44: 463-472.
- VERMEULEN, S.J., BRUYNEEL, E.A., BRACKE, M.E., DE BRUYNE, G.K., VENNEKENS, K.M., VLEMINCKX, K.L., BERX, G.J., VAN ROY, F.M. and MAREEL, M.M. (1995). Transition from the noninvasive to the invasive phenotype and loss of α -catenin in human colon cancer cells. *Cancer Res* 55: 4722-4728.
- VLEMINCKX, K., VAKAET, L. Jr, MAREEL, M., FIERS, W. and VAN ROY, F. (1991). Genetic manipulation of E-cadherin expression by epithelial tumor cells reveals an invasion suppressor role. *Cell* 66: 107-119.
- WANG, F., HANSEN, R.K., RADISKY, D., YONEDA, T., BARCELLOS-HOFF, M.H., PETERSEN, O.W., TURLEY, E.A. and BISSELL, M.J. (2002). Phenotypic reversion or death of cancer cells by altering signaling pathways in three-dimensional contexts. *J Natl Cancer Inst* 94: 1494-1503.
- WOLF, K., MAZO, I., LEUNG, H., ENGELKE, K., VON ANDRIAN, U.H., DERYUGINA, E.I., STRONGIN, A.Y., BRÖCKER, E.-B. and FRIEDL, P. (2003). Compensation mechanism in tumor cell migration: mesenchymal-amoeboid transition after blocking of pericellular proteolysis. *J Cell Biol* 160: 267-277.

Further Related Reading, published previously in the *Int. J. Dev. Biol.*

See Special Issue ***Pattern Formation*** edited by Michael K. Richardson and Cheng-Ming Chuong at:
<http://www.ijdb.ehu.es/web/contents.php?vol=53&issue=5-6>

Parallels in invasion and angiogenesis provide pivotal points for therapeutic intervention

Suzanne A. Eccles
Int. J. Dev. Biol. (2004) 48: 583-598

The «chemoinvasion assay»: a tool to study tumor and endothelial cell invasion of basement membranes

Adriana Albini, Roberto Benelli, Douglas M. Noonan and Claudio Brigati
Int. J. Dev. Biol. (2004) 48: 563-571

Germinal tumor invasion and the role of the testicular stroma

Alejandro Díez-Torre, Unai Silván, Olivier De Wever, Erik Bruyneel, Marc Mareel and Juan Aréchaga
Int. J. Dev. Biol. (2004) 48: 545-557

The countercurrent principle in invasion and metastasis of cancer cells. Recent insights on the roles of chemokines

Ghislain Opendakker and Jo Van Damme
Int. J. Dev. Biol. (2004) 48: 519-527

The stroma reaction myofibroblast: a key player in the control of tumor cell behavior

Alexis Desmoulière, Christelle Guyot and Giulio Gabbiani
Int. J. Dev. Biol. (2004) 48: 509-517



5 yr ISI Impact Factor (2008) = 3.271

